Available online at www.sciencedirect.com
SCIENCE DIRECT®
Journal of Sound and Vibration 276 (2004) 335–359
JOURNAL OF SOUND AND VIBRATION
www.elsevier.com/locate/jsvi

The Global Transfer Direct Transfer method applied to a finite simply supported elastic beam

O. Guasch*, F.X. Magrans

ICR, Ingeniería para el Control del Ruido S.L., C/Berruguete no 52, Barcelona 08 035, Spain

Received 18 September 2002; accepted 22 July 2003

Abstract

The Global Transfer Direct Transfer (GTDT) method is a two-step transmission path analysis method. It is used to analyze the signal transmission among subsystems from a general N-dimensional linear network, representing the physical model under study. In the first step, the Global Transfer Functions (GTFs) are measured and the Direct Transfer Functions (DTFs) are calculated from them. In the second step, the signal vector is measured for the network running under the desired operational conditions. It is then possible to reconstruct the signal in any subsystem from the contributions of all other subsystems plus its own external excitation. This is done by means of the previously calculated DTFs.

This paper is intended to clarify how the GTDT method works. This is done by means of an analytic study of the bending wave transmission between three points in a finite simply supported elastic beam. This problem constitutes a particular four-dimensional example of the general N-dimensional network. Concerning the first step of the method, special emphasis is given to the relationship among the DTFs and the GTFs, as well as to elucidate the role of the DTF matrix as a connectivity matrix. As for the second step of the method, the particular case of a correlated force vector acting on the beam is addressed. It is shown how the signal at any subsystem can be reconstructed from the signals at all the other subsystems. In practical implementations this allows to identify problematic subsystems in order to perform appropriate design modifications and avoids the necessity of having to measure operational forces.

1. Introduction

In the past three decades, several methods have been developed to deal with the problem of analyzing noise and vibration transmission paths in physical systems. These methods are

*Corresponding author. Tel./fax: +34-93-428-63-39.
E-mail address: oguasch@icrsl.com (O. Guasch).

0022-460X/$ - see front matter
doi:10.1016/j.jsv.2003.07.032

generically known as Transmission Path Analysis (TPA) methods. The physical systems under study can often be schematically modelled by a linear network of N connected subsystems. The various TPA methods then analyze different types of relationships among these subsystems: relations among the forces acting on them and the subsystem signals, relations among the signals themselves, paths followed by the signals from one subsystem to another, etc.

A general distinction can be made between the so-called one-step methods and the two-step methods. The former extract information from the measured operational forces and signals. See for instance the Multiple Input Single/Multiple Output (MISO–MIMO) methods (Refs. [1–5] and Ref. [6] for comparison). The latter measure transfer functions in a first step, with the network stationary, and obtain the final results from a second set of measurements with the network running under the desired operational conditions. Examples of two-step methods are the Global Transfer Direct Transfer (GTDT) method [7] or the Force Transfer Functions (FTF) methods (e.g., Refs. [7–9]).

This paper focuses on some features of the GTDT method. This method was developed in Ref. [7] to deal with the case of a linear N-dimensional network under steady operational conditions and then extended to non-steady cases [10] showing a large resemblance with the Markov chains theory when used to describe phonon random walks in closed spaces [11]. A Statistical Energy Analysis (SEA) implementation of the method was also carried out [12] and a recent easy-to-handle matrix formulation has been carried out. The transmission path analysis approach in Ref. [12] can also be found in Ref. [13]. It is worthwhile to mention that similar ideas to those presented by the GTDT method have been independently developed in different fields such as neurology [14] or economy [15].

One of the cornerstones of the GTDT method, found in its first step, concerns the relationship between the Global Transfer Functions (GTFs) and the Direct Transfer Functions (DTFs). The former correspond to the common concept of a measurable transfer function, i.e., they give the quotient between the signal at a subsystem j and the signal, or the force, at a subsystem i when i is excited. The latter represent, roughly speaking, the quotient between the signals at j and i when i is excited and all the other subsystems in the network remain somehow blocked. Consequently, the DTFs cannot be measured and have to be calculated from the GTFs. It is one of the purposes of this paper to help clarify the differences between both types of transfer functions and the calculations involved in obtaining the DTFs. Another objective is to show that the direct transfer matrix (built from all DTFs among subsystems) plays the role of a connectivity matrix, i.e., the elements corresponding to straight-linked subsystems are non-zero while subsystems linked through a third one have a zero DTF.

The other cornerstone of the GTDT method is found in its second step. It concerns the operational signal reconstruction in any subsystem by means of the DTFs and the operational signals in all the other network subsystems. This allows one to identify problematic subsystems and gives a tool to predict how a design modification in one subsystem can diminish the signal of any other one (this can obviously be done if it is possible to estimate the new DTFs and/or the subsystem signals reduction which is often the case in many practical situations). The method also avoids the necessity of having to measure operational forces. In this paper, attention will be focused on how the signal reconstruction is to be carried out for the particular case of a correlated force vector acting on the system. The meaning of the so-called external signal will also be addressed.

The above concepts will be dealt with by means of the analytic study of the bending wave transmission between three points in a finite simply supported elastic beam. This example corresponds to a particular four-dimensional case of the general N-dimensional one. The paper is thus focused on some theoretical features of the method. Consequently, no mention will be made, for instance, of how the various subsystems have to be selected in practical cases. The different ways of how measurements are to be made for the correlated and energetic cases as well as the benefits that can be obtained from subsystem design modifications are not addressed here. These subjects will be presented in subsequent work on industrial applications of the GTDT method.

Concerning the terminology used throughout the paper, it has to be mentioned that the term subsystem has been identified with a single degree of freedom (d.o.f). Taking into account that in industrial applications one single d.o.f will often be intended to represent the behaviour of an entire physical entity (e.g., r.m.s. normal velocity of a plate under the SEA hypothesis, one-point normal velocity of a plate vibrating in an eigenmode or in a simple combination of eigenmodes), it has become quite customary to identify the d.o.f itself with the physical entity it represents (usually referred to as a subsystem, e.g., in SEA). Under these assumptions, it is not contradictory to use the term subsystem to designate the d.o.f. Although this is not the case for the example presented here because only one physical entity will be considered (the beam) while 4 d.o.f. will be taken into account, the term subsystem to designate each d.o.f has been kept to follow the terminology used in related work on the GTDT method (see Refs. [7,10,12]). On the other hand note that transfer functions only make full sense when defined between d.o.f and not between physical entities.

The paper is organized as follows. In Section 2 a brief overview of the GTDT method for an N-dimensional linear network is presented. Section 3 states the analytical problem of bending wave transmission in a simply supported elastic beam within the GTDT framework. Section 4 calculates the GTFs among all subsystems. In Section 5 the DTFs are calculated from the previously obtained GTFs and the role of the DTF matrix as a connectivity matrix is shown. In Section 6, the signal reconstruction at any subsystem by means of the signals at the remaining ones is carried out. Conclusions are finally given in Section 7.

2. The GTDT method: a brief overview

2.1. Motivation of the method

Consider, as an example, the vibration transmission from the bogie of a railway carriage to the noise at its interior. A network of subsystems modelling the carriage behaviour could be built, for instance, from the three axes accelerations (displacements or velocities) at the bogie connection points, the normal accelerations of the carriage inner panels and the acoustic pressure at a control microphone inside the carriage. Suppose a simplified and idealized case with only two bogie connection points where accelerations in just one axis remain of interest, four interior panels (floor, two laterals and roof) with their corresponding normal accelerations and the acoustic pressure at one microphone. That makes a total of 7 subsystems that form the discrete system representing the continuous physical one (railway carriage). The seven-dimensional network in Fig. 1 can schematically represent the connectivity among these subsystems. As seen, it is assumed

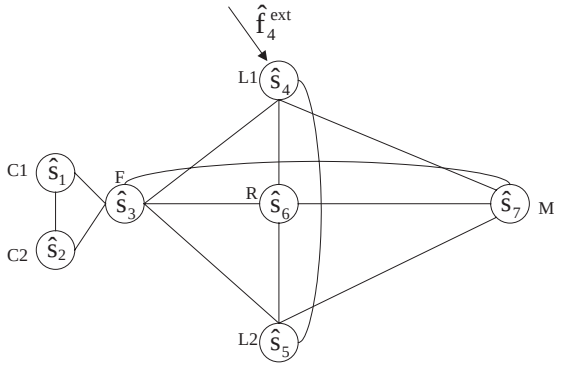

Fig. 1. Railway carriage example. C1: Connection point 1, C2: Connection point 2, F: Floor, L1: Lateral 1, L2: Lateral 2, R: Roof, M: Microphone inside the carriage.

that there is no airborne noise paths or links from the connection points C1 and C2 to the interior microphone M, i.e. an impact hammer at C1 only generates sound at M as long as it induces vibrations on subsystems F, L1, L2 and R that are directly connected to M.

Consider what happens, for instance, if the force–acoustic pressure and the acceleration–acoustic pressure transfer functions from L1 to M in Fig. 1 are to be measured. In the first case, an impedance hammer can be used to excite L1 and measure the force, while at the same time a microphone measures the acoustic pressure at M. The force–acoustic pressure transfer function is then obtained, as usual, by dividing the signal at M by the force at L1 in the frequency domain (no comments will be made here of the statistics involved in the measurement process). However, notice that the acoustic pressure measured at M is not only due to the noise generated by the vibration of L1 induced by the hammer impact on it, but to the vibration of all the other subsystems of the network directly connected to M, i.e., R, L2 and F. These subsystems are also linked to L1 and thus will be excited by the impact on it. In turn, the vibrations of these subsystems will actually depend on the response of the whole network (C1, C2, F, L1, L2, R, M) to the impact at L1. Since each subsystem has been independently excited, the superposition principle can be used to obtain the subsystem force contributions to the acoustic pressure at M in the second step of the method. However, these contributions do not represent independent transmission paths or links since the signal at M after each excitation is due to the response of the entire network. The situation gets even more intricate if an acceleration–acoustic pressure transfer function is used. In this case an accelerometer can be placed at L1 and a hammer used to excite it. The transfer function will be again obtained by dividing the signal at M, which is due to the vibrations of all the coupled subsystems, by the acceleration at L1, which is generated from the combination of the impact at L1 plus the response from all the other subsystems to it. Moreover, given that it is not feasible to cause an acceleration at L1 without producing an acceleration at any other subsystem (the same remaining true if the acceleration is generated at any other subsystem C1, C2, F, L1, L2, R), it is impossible to obtain a set of independent measured transfer functions to which the superposition principle can be applied. Therefore, in the second step of the method it would not be possible to readily obtain the contributions from the subsystem overall accelerations to the acoustic pressure at M in terms of the measured transfer functions. Note, however, that it is

possible to apply the superposition principle to these transfer functions if only the fractions of the accelerations due to the external excitations at each subsystem are considered.

These types of transfer functions (force–acoustic pressure, acceleration–acoustic pressure, force–acceleration and acceleration–acceleration in the above example), which are the only ones that can be measured without modifying the system under study, are termed Global Transfer Functions (GTFs) in the GTDT method of transmission paths analysis. The name comes from the fact that the signal is transmitted from the excited subsystem to the receiver subsystem taking into account any link between them. The set of all these paths or links is termed a *global* transmission path in the GTDT framework

In view of the above considerations, it would be interesting to obtain the transfer function between L1 and M when the signal at the remaining subsystems is zero, i.e., the signal is only transmitted from L1 to M through the direct path or link connecting them while the other subsystems remain somehow blocked. These ''ideal'' transfer functions are termed Direct Transfer Functions (DTFs) in the GTDT method and are not measurable quantities. However, the DTFs can be calculated once the GTFs have been measured. The term *direct* comes from the fact that in this case the signal is only transmitted from the excited subsystem to the receiver following the direct link between them. The advantages of using the DTFs are two-fold. First, they constitute an independent set of transfer functions where the superposition principle in the second step of the method can be applied, if signal–signal transfer functions are used for the signal reconstruction at any subsystem. Second, they allow one to get individual transmission paths among subsystems by obtaining independent links among them. This becomes especially appealing, for instance, when design modifications are to be performed and it is necessary to know how changes in one subsystem may affect another one without considering the whole system.

On the other hand, notice that in the railway carriage example, the DTF from L1 to M will be non-zero but the DTFs from C1 to M will be zero, as there is no direct link between C1 and M (see Fig. 1). The same holds for the DTF between C2 and M.

The second step of the GTDT method consists in using the DTFs to reconstruct the operational signal at any subsystem from the external signal acting on it plus the operational signals at the remaining subsystems. On one hand this avoids the necessity of having to measure operational forces. Moreover, these forces cannot always be controlled in order to reduce their effect on a desired subsystem. In the railway carriage example, for instance, forces of very different nature will generate noise inside the carriage. Some of these forces will be due to the rail/wheel interaction, to the rail discontinuities, to the aerodynamic loading or to the engine and auxiliary equipment connections to the carriage. Although the influence of some of them on the noise at M can sometimes be reduced this will not be generally the case. However, if the signal at M is known in terms of the direct signal contributions of subsystems F, L1, L2 and R, it is possible to estimate, for instance, how a design modification at L2 (e.g., a change in thickness or in rigidity, a double panel) will increase or diminish its vibration and its new effect on the noise at M. That is to say, once the new DTF between L2 and M is obtained, it is possible to see how the modification on L2 influences the noise measured at M, without taking into consideration the subsystems that are not directly linked to them. In fact, this is the final motivation of the GTDT method, i.e., to detect problematical subsystems and see how design modifications may help to reduce noise at a given location.

2.2. Relationship among DTFs and GTFs: the general case

In what follows a more rigorous definition of a GTF and a DTF in a general N-dimensional network will be given. However, the reader is referred to Ref. [7] for further details, comments and discussions. Again, no mention will be made of the statistical process involved in the GTFs measurements.

The external *force vector* acting on the N-dimensional network will be denoted by $\hat{\mathbf{f}}^{ext}(\omega) = (\hat{f}_1^{ext}(\omega), \hat{f}_2^{ext}(\omega), \cdots, \hat{f}_N^{ext}(\omega))^{\mathrm{T}}$ while $\hat{\mathbf{s}}(\omega) = (\hat{s}_1(\omega), \hat{s}_2(\omega), \cdots, \hat{s}_N(\omega))^{\mathrm{T}}$ will denote the corresponding measured *signal vector*. Each component, $\hat{f}_i^{ext}(\omega)$, of the force vector can represent different physical quantities such as forces or moments. The same remains valid for the signal vector where $\hat{s}_i(\omega)$ can represent quantities such as acceleration, velocity, displacement, acoustic pressure, etc.

The GTF between two subsystems i and j, $\hat{T}_{ij}^{G}(\omega)$, is defined as the quotient between the signal at j, $\hat{s}_j(\omega)$, and the signal at i, $\hat{s}_i(\omega)$, when there is only one non-zero and independent external excitation, $\hat{f}_i^{ext}(\omega)$, applied to i which has been transmitted to j via a global path:

$$\hat{T}_{ij}^{G}(\omega) = \frac{\hat{s}_j(\omega)}{\hat{s}_i(\omega)} \quad \text{with } \hat{\mathbf{f}}^{ext}(\omega) = (0, \cdots, 0, \hat{f}_i^{ext}(\omega), 0, \cdots, 0)^{\mathrm{T}} \tag{1}$$

As mentioned, (1) coincides with the usual definition of a transfer function. Note that for a signal–signal transfer function with the same physical magnitude in both, the numerator and denominator, it follows that $\hat{T}_{ii}^{G}(\omega) = 1 \quad \forall i = 1 \cdots N$. On the other hand if $\hat{s}_i(\omega)$ is replaced by $\hat{f}_i^{ext}(\omega)$ a force–signal transfer function is obtained.

The DTF, $\hat{T}_{ij}^{D}(\omega)$, from subsystems i to j, with $i \neq j$, is defined as the quotient between the signal at j, $\hat{s}_j(\omega)$, and the signal at i, $\hat{s}_i(\omega)$, when a non-zero and independent external excitation, $\hat{f}_i^{ext}(\omega)$, applied to i that has been transmitted to j via a direct path, i.e., all other signals $\hat{s}_k(\omega)$, with $k \neq i, j$ remain zero:

$$\hat{T}_{ij}^{D}(\omega) = \frac{\hat{s}_j(\omega)}{\hat{s}_i(\omega)} \quad \text{with } \hat{s}_k(\omega) = 0 \quad \forall k \neq i, j. \tag{2}$$

As already mentioned, the DTF between two points gives the quotient of their signals when all the other subsystems in the network remain somehow blocked, i.e. their signals are zero.

Finally, the DTF, $T_{ii}^{D}(\omega)$, from a subsystem i to itself, is defined as the quotient between the signal at i, $\hat{s}_i(\omega)$, when there is only one non-zero and independent external excitation $\hat{f}_i^{ext}(\omega)$ applied to i, and all the other signals $\hat{s}_k(\omega)$ with $k \neq i$ remain zero, and the signal at i, $\hat{s}_i^{ext}(\omega)$, when the same external excitation $\hat{f}_i^{ext}(\omega)$ is applied to i and there is no restriction on the other subsystem signals (i.e., the signal can be transmitted back to i via a global path):

$$\hat{T}_{ii}^{D}(\omega) = \frac{\hat{s}_i'(\omega)}{\hat{s}_i^{ext}(\omega)}, \tag{3a}$$

where

$$\hat{s}_i'(\omega) = \hat{s}_i(\omega) \quad \text{if } \hat{\mathbf{s}}(\omega) = (0, \cdots, 0, \hat{s}_i(\omega), 0, \cdots, 0)^{\mathrm{T}} \tag{3b}$$

and $\hat{s}_i^{ext}(\omega)$ is the ith component of $\hat{\mathbf{s}}(\omega)$ when there is no restriction of nullity on all other components $j \neq i$, i.e.

$$\hat{s}_i^{ext}(\omega) = \hat{s}_i(\omega) \text{ signal at } i \text{ if} \begin{cases} \hat{\mathbf{f}}^{ext}(\omega) = (0, \cdots, 0, \hat{f}_i^{ext}(\omega), 0, \cdots, 0)^{\mathrm{T}}, \\ \hat{\mathbf{s}}(\omega) = (\hat{s}_1(\omega), \hat{s}_2(\omega), \cdots, \hat{s}_i(\omega), \cdots, \hat{s}_N(\omega))^{\mathrm{T}}. \end{cases} \tag{3c}$$

The notation $\hat{s}_i^{ext}(\omega)$ accounts for the fact that (3c) represents the overall signal at i that is caused by the external excitation applied on i plus the response contributions of all other subsystems j, with $j \neq i$, to this excitation. Consequently, $\hat{s}_i'(\omega) = \hat{T}_{ii}^D(\omega)\hat{s}_i^{ext}(\omega)$ represents the fraction of $\hat{s}_i^{ext}(\omega)$ that is only due to the external excitation on i. As opposed to the signal–signal GTFs, $\hat{T}_{ii}^D(\omega) \neq 1$. Note that neither $T_{ii}^D(\omega)$ nor $\hat{s}_i'(\omega)$ nor $\hat{s}_i^{ext}(\omega)$ are measurable quantities.

Applying Eq. (1) to all pairs of subsystems in the network, a global transfer matrix $\hat{\mathbf{T}}^G$ can be built. In the same way, from (2) and (3a) a direct transfer matrix $\hat{\mathbf{T}}^D$ can be built, Eq. (2) giving its off-diagonal elements and Eq. (3a) the diagonal ones. The DTFs and GTFs matrices can then be related through the equation

$$\hat{\mathbf{T}}^G\hat{\mathbf{T}}^{DE} = -\mathbf{\Lambda}_{TD}, \tag{4}$$

where $\hat{\mathbf{T}}^{DE} = \operatorname{dev}\hat{\mathbf{T}}^D - \mathbf{I}$, being $\mathbf{I}$ the identity matrix and $\operatorname{dev}\hat{\mathbf{T}}^D$ the deviatoric part of $\hat{\mathbf{T}}^D$ defined as

$$\operatorname{dev}\hat{\mathbf{T}}^D|_{ij} = \hat{T}_{ij}^D(\omega)(1-\delta_{ij}), \tag{5}$$

where δ_{ij} is the Kronecker delta. $\mathbf{\Lambda}_{TD}$ is the diagonal matrix whose non-zero elements are given by (3a)

$$\mathbf{\Lambda}_{TD}|_{ij} = \hat{T}_{ij}^D(\omega)\delta_{ij}. \tag{6}$$

Eq. (4) can be used to obtain the $\hat{\mathbf{T}}^D$ matrix from the inverse of the $\hat{\mathbf{T}}^G$ matrix. From (4) it follows that

$$-\hat{\mathbf{T}}^{DE}\mathbf{\Lambda}_{TD}^{-1} = (\hat{\mathbf{T}}^G)^{-1} \tag{7}$$

and taking into account that

$$-\hat{\mathbf{T}}^{DE}\mathbf{\Lambda}_{TD}^{-1}\Big|_{ii} = 1/T_{ii}^D(\omega), \tag{8a}$$

$$-\hat{\mathbf{T}}^{DE}\mathbf{\Lambda}_{TD}^{-1}\Big|_{ij} = -T_{ij}^D(\omega)/T_{ii}^D(\omega), \quad i \neq j \tag{8b}$$

it is straightforward to find $\hat{\mathbf{T}}^D$.

2.3. Signal reconstruction from DTFs and GTFs

In order to find the operational signal in any subsystem in terms of the external signal acting on it and the remaining subsystem operational signals, the former has to be first obtained. This can be done because the external signal vector, $\hat{\mathbf{s}}^{ext}(\omega)$, can be calculated from measurable quantities such as the operational signal vector $\hat{\mathbf{s}}(\omega)$ and the GTF matrix $\hat{\mathbf{T}}^G$. From equations in Ref. [7] written in matrix form, it follows that:

$$\hat{\mathbf{s}}^{ext} = (\hat{\mathbf{T}}^{G^{\mathrm{T}}})^{-1}\hat{\mathbf{s}}. \tag{9}$$

The signal vector, $\hat{\mathbf{s}}(\omega)$, is then related to $\hat{\mathbf{s}}^{ext}(\omega)$ and $\hat{\mathbf{T}}^D$ by means of

$$\hat{\mathbf{s}} = (\operatorname{dev}\hat{\mathbf{T}}^D)^{\mathrm{T}}\hat{\mathbf{s}} + \mathbf{\Lambda}_{TD}\hat{\mathbf{s}}^{ext}. \tag{10}$$

Notice that as the deviatoric part of $\hat{\mathbf{T}}^D$ appears in (10), $\hat{s}_i(\omega)$ is expressed in terms of $\hat{s}_j(\omega)\ \ \forall j \neq i$ and $\hat{s}_i^{ext}(\omega)$.

In the following sections, the concepts developed above will be applied to the particular case of bending wave transmission in a finite simply supported elastic beam.

3. Statement of the beam example

Consider the case of a simply supported Euler–Bernouilli beam of length L. The chosen subsystems are the vertical displacements at three arbitrary points $\{x_1, x_2, x_3\} \in \Omega = [0, L]$ with $x_1 < x_2 < x_3$ and the angle rotated at the point x_2 (see Table 1, Fig. 2a). That makes a total of 4 subsystems so that the beam problem to be dealt with corresponds to a particular example of a four-dimensional linear network. On the other hand, the two boundary points of the beam are denoted by $\partial\Omega = \{x = 0, x = L\}$.

The components of the (4×4) global transfer matrix, $\hat{\mathbf{T}}^G$, will be first obtained and from it the corresponding (4×4) direct transfer matrix $\hat{\mathbf{T}}^D$. *The main result, concerning the first step of the GTDT method, will be that unlike the GTFs* $\hat{T}^G_{14}$ *and* $\hat{T}^G_{41}$, *which are non-zero, the DTFs* $\hat{T}^D_{14} = \hat{T}^D_{41} = 0$, i.e., *these DTFs quantify the well-known fact that no signal can be transmitted from* x_1 *to* x_3 *if neither a displacement nor a rotation are allowed at* x_2. On the contrary, all remaining GTFs and DTFs will be non-zero. Hence, *the DTF matrix plays the role of a connectivity matrix among subsystems*. The situation is schematically shown in Fig. 2b, where the connectivity graphs for the global and direct transfer functions associated to the beam problem are shown.

In order to first obtain the global transfer functions, $\hat{T}^G_{ij}$, the inhomogeneous differential equations governing the bending vibrations of the beam for a point harmonic force and a point harmonic moment excitations have to be considered. The solutions to these equations will correspond to force–displacement and moment–displacement transfers functions (receptances in the mechanics field), from which force–angle and moment–angle transfer functions can be easily derived too. Although it is also possible to apply the first step of the GTDT methodology to these types of transfer functions, signal–signal transfers functions (displacement–displacement, displacement–angle and angle–displacement) will be used, as in the original formulation [7]. The signal–signal GTFs can be obtained by forming ratios of the various force–displacement/angle and moment–displacement/angle GTFs. However, it has to be pointed out that this procedure is only valid because analytic expressions are used for all the involved transfer functions. In case of the force–displacement GTFs being obtained by means of measurements, and thus involving a statistical process, this operation will be totally incorrect. In such a case (the most usual one in practical applications of TPA methods) it is necessary to directly measure the

Table 1
Beam subsystems

Subsystem number	Variable description	Variable
1	Vertical displacement	$U(x_1)$
2	Vertical displacement	$U(x_2)$
3	Angle of rotation	$W(x_2)$
4	Vertical displacement	$U(x_3)$

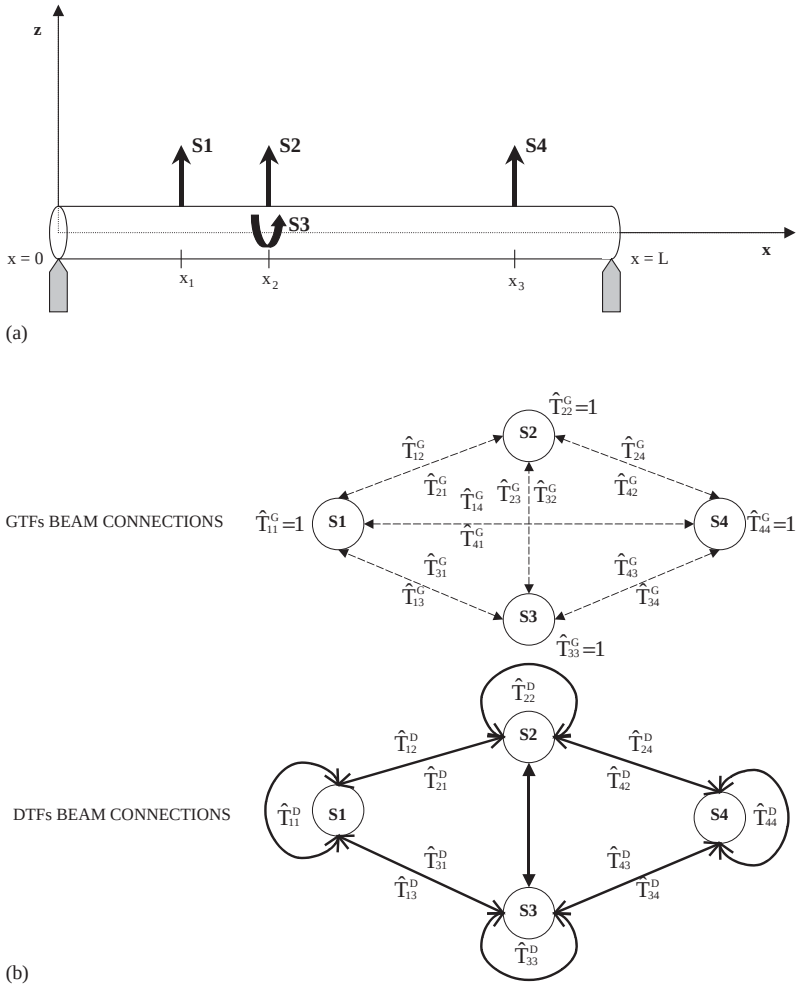

Fig. 2. (a) Subsystems location in the beam and (b) GTFs and DTFs networks corresponding to Fig 2a.

signal–signal transfer functions. On the other hand and regardless of the procedure used to obtain the GTFs, the DTFs will be obtained from them by means of Eqs. (8a) and (8b).

With regards to the second step of the method, the main result will be that *the DTFs can be used to reconstruct the operational signal at any subsystem i*, $\hat{s}_i(\omega)\ \ \forall i = 1, \cdots, 4$, *from the external signal acting on i,* $\hat{s}_i^{ext}(\omega)$, *and the operational signals at the remaining subsystems* $\hat{s}_j(\omega)\ \ \forall j \neq i$. In order to do so, a correlated force vector will be assumed to be acting on the beam. The corresponding signal vector will then be calculated by means of the cross-receptance matrix. These two vectors (force and signal), are to be viewed respectively as measured quantities in practical applications of the Force Transfer Functions (FTF) and GTDT methods. If the signal in any subsystem is reconstructed in terms of the forces acting on the system, $\hat{\mathbf{f}}^{ext}(\omega)$, and by means of the global receptance matrix, the procedure will correspond to the FTF method. On the other hand, if the signal in any subsystem is reconstructed from the external signal acting on it, $\hat{\mathbf{s}}^{ext}(\omega)$, the signals of

all the other subsystems, $\hat{\mathbf{s}}(\omega)$, and by means of the direct transfer matrix, the procedure will correspond to the GTDT method. The results of both approaches will be shown for the beam example.

4. The global transfer functions

4.1. Force excitation

The inhomogeneous differential equation governing the bending vibrations of a finite elastic beam for the case of a unit value force applied at a concentrated point x_0 is given by (see, e.g., Refs. [16,17]).

$$B\partial_x^4 u_F + \rho S\partial_t^2 u_F = \delta(x - x_0), \tag{11}$$

where $B = EI$ is the bending stiffness, E is Young's modulus and I is the second moment of area. ρ is the beam density and S is the cross-sectional area. u_F denotes the vertical displacement (see Fig. 2a) while $\partial_x^4 u_F$ and $\partial_t^2 u_F$, respectively, denote the displacement fourth order space derivative and the displacement second order time derivative. Performing the Fourier transform of (11) and defining $k = (\rho S\omega^2/B)^{1/4}$ yields

$$\partial_x^4 \hat{U}_F - k^4 \hat{U}_F = \delta(x - x_0). \tag{12}$$

The solution to (12) is commonly known as the time-independent Green function for the linear differential equation at hand. The Green function is termed the *exact* Green function for a particular problem if it also satisfies the boundary conditions associated with it (see, e.g., Ref. [18]). This Green function for the simply supported beam (force cross-receptance between x_0 and x) is given by (see Appendix A):

$$\begin{aligned}\hat{U}_F(x, x_0) &\equiv G(x, x_0)\\ &= \frac{1}{2k^3}\begin{cases} \dfrac{\sinh(k(x_0 - L))}{\sinh(kL)}\sinh(kx) - \dfrac{\sin(k(x_0 - L))}{\sin(kL)}\sin(kx), & x < x_0,\\ \dfrac{\sinh(kx_0)}{\sinh(kL)}\sinh(k(x - L)) - \dfrac{\sin(kx_0)}{\sin(kL)}\sin(k(x - L)), & x > x_0. \end{cases}\end{aligned} \tag{13}$$

Function (13) satisfies the symmetry relationship $G(x, x_0) = G(x_0, x)$ as well as the boundary conditions of the problem. It can also be easily checked that (13) is the solution of the differential Eq. (12).

On the other hand, the angle, $\hat{W}_F(x, x_0)$, rotated at a point x due to a point excitation at x_0 can be straightforwardly obtained taking into account that $\hat{W}_F(x, x_0) = \partial_x \hat{U}_F(x, x_0)$. It follows from (13) that

$$\hat{W}_F(x, x_0) = \frac{1}{2k^2}\begin{cases} \dfrac{\sinh(k(x_0 - L))}{\sinh(kL)}\cosh(kx) - \dfrac{\sin(k(x_0 - L))}{\sin(kL)}\cos(kx), & x < x_0,\\ \dfrac{\sinh(kx_0)}{\sinh(kL)}\cosh(k(x - L)) - \dfrac{\sin(kx_0)}{\sin(kL)}\cos(k(x - L)), & x > x_0. \end{cases} \tag{14}$$

4.2. Moment excitation

The displacement (in the frequency domain) at a point x when a concentrated moment excitation acts at point x_0 is given by the solution of the following inhomogeneous equation for the beam

$$\partial_x^4 \hat{U}_M - k^4 \hat{U}_M = \partial_x \delta(x - x_0). \tag{15}$$

The solution to (15) for the simply supported beam (moment cross-receptance between x_0 and x) is given by (see Appendix B):

$$\begin{aligned} &\hat{U}_M(x, x_0) \\ &\quad = -\partial_{x_0} G(x, x_0) \\ &\quad = \frac{1}{2k^2} \begin{cases} -\dfrac{\cosh(k(x_0 - L))}{\sinh(kL)} \sinh(kx) + \dfrac{\cos(k(x_0 - L))}{\sin(kL)} \sin(kx), & x < x_0, \\ -\dfrac{\cosh(kx_0)}{\sinh(kL)} \sinh(k(x - L)) + \dfrac{\cos(kx_0)}{\sin(kL)} \sin(k(x - L)), & x > x_0. \end{cases} \end{aligned} \tag{16}$$

The angle, $\hat{W}_M(x, x_0)$, rotated at a point x due to a concentrated moment excitation at x_0 can be obtained again taking into account that $\hat{W}_M(x, x_0) = \partial_x \hat{U}_M(x, x_0)$. Then it follows from (16) that

$$\hat{W}_M(x, x_0) = \frac{1}{2k} \begin{cases} -\dfrac{\cosh(k(x_0 - L))}{\sinh(kL)} \cosh(kx) + \dfrac{\cos(k(x_0 - L))}{\sin(kL)} \cos(kx), & x < x_0, \\ -\dfrac{\cosh(kx_0)}{\sinh(kL)} \cosh(k(x - L)) + \dfrac{\cos(kx_0)}{\sin(kL)} \cos(k(x - L)), & x > x_0. \end{cases} \tag{17}$$

4.3. The beam global transfer functions

From (13), (14), (16) and (17), it is possible to build all displacement–displacement, displacement–angle and angle–displacement GTFs carrying out the appropriate ratios. It is again remarked that dividing, for instance, force–displacement transfer functions in order to obtain displacement–displacement transfer functions is only allowed because analytic expressions are known for them and no statistics are involved.

On the other hand, observe that all functions $\hat{U}_F(x, x_0)$, $\hat{W}_F(x, x_0)$, $\hat{U}_M(x, x_0)$ and $\hat{W}_M(x, x_0)$ are continuous at $x = x_0$, so the transfer functions are well defined at this point. Respectively, denoting with superscripts $>$ and $<$ the solutions for $x > x_0$ and $x < x_0$ and taking into account that any of them can be used for the solution at $x = x_0$ due to continuity, the transfer functions

are given by

$$\begin{array}{cccc}
\hat{T}^G_{11}=1, & \hat{T}^G_{12}=\dfrac{\hat{U}^{>}_F(x_2,x_1)}{\hat{U}_F(x_1,x_1)}, & \hat{T}^G_{13}=\dfrac{\hat{W}^{>}_F(x_2,x_1)}{\hat{U}_F(x_1,x_1)}, & \hat{T}^G_{14}=\dfrac{\hat{U}^{>}_F(x_3,x_1)}{\hat{U}_F(x_1,x_1)},\\
\hat{T}^G_{21}=\dfrac{\hat{U}^{<}_F(x_1,x_2)}{\hat{U}_F(x_2,x_2)}, & \hat{T}^G_{22}=1, & \hat{T}^G_{23}=\dfrac{\hat{W}_F(x_2,x_2)}{\hat{U}_F(x_2,x_2)}, & \hat{T}^G_{24}=\dfrac{\hat{U}^{>}_F(x_3,x_2)}{\hat{U}_F(x_2,x_2)},\\
\hat{T}^G_{31}=\dfrac{\hat{U}^{<}_M(x_1,x_2)}{\hat{W}_M(x_2,x_2)}, & \hat{T}^G_{32}=\dfrac{\hat{U}_M(x_2,x_2)}{\hat{W}_M(x_2,x_2)}, & \hat{T}^G_{33}=1, & \hat{T}^G_{34}=\dfrac{\hat{U}^{>}_M(x_3,x_2)}{\hat{W}_M(x_2,x_2)},\\
\hat{T}^G_{41}=\dfrac{\hat{U}^{<}_F(x_1,x_3)}{\hat{U}_F(x_3,x_3)}, & \hat{T}^G_{42}=\dfrac{\hat{U}^{<}_F(x_2,x_3)}{\hat{U}_F(x_3,x_3)}, & \hat{T}^G_{43}=\dfrac{\hat{W}^{<}_F(x_2,x_3)}{\hat{U}_F(x_3,x_3)}, & \hat{T}^G_{44}=1,
\end{array} \tag{18}$$

where the following symmetries apply:

$$\hat{U}_F(x_0,x)=\hat{U}_F(x,x_0),\quad \hat{W}_M(x_0,x)=W_M(x,x_0)\quad\text{and}\quad -\hat{W}_F(x_0,x)=\hat{U}_M(x,x_0),$$

The above considered GTFs (18) also represent velocity–velocity, velocity–angular velocity and angular velocity–velocity transfer functions (read also acceleration–acceleration, acceleration–angular acceleration and angular acceleration–acceleration) given that a cancelled factor $\partial_t^n \leftrightarrow (\mathrm{i}\omega)^n$ with $n=1,2$, would appear both in the numerator and denominator of the GTFs in (18).

5. The direct transfer functions

Section 2 showed that the DTFs can be obtained from the GTFs by means of Eq. (7). The main purpose of this section is to see that $\hat{T}^D_{14}=\hat{T}^D_{41}=0$ while $\hat{T}^D_{ij}\neq 0$ for $i,j=1,\ldots,3$ and for $i,j=2,\ldots,4$. Taking into account Eq. (7) and relationships (8a) and (b), it will suffice to prove that

$$(\hat{\mathbf{T}}^G)^{-1}|_{14}=(\hat{\mathbf{T}}^G)^{-1}|_{41}=0, \tag{19a}$$

$$(\hat{\mathbf{T}}^G)^{-1}|_{ii}<\infty,\quad (\hat{\mathbf{T}}^G)^{-1}|_{ij}\neq 0\quad i,j=1,\ldots,3,\quad i,j=2,\ldots,4 \text{ with } i\neq j. \tag{19b}$$

As mentioned in Ref. [7], for the problem to be well defined it is first required that $\det(\hat{\mathbf{T}}^G)\neq 0$. This is the case for real physical systems that always have a certain amount of damping but it fails at the eigenfrequencies of ideal non-damped systems. This can be seen in Fig. 3, where the logarithm of $\det(\hat{\mathbf{T}}^G)$ is plotted against frequency. The determinant of $\hat{\mathbf{T}}^G$ vanishes for $f_1\approx 32.5$ Hz, $f_2\approx 130.1$ Hz and $f_3\approx 292.6$ Hz, which are the eigenfrequencies for the simply supported beam in the [0, 500] Hz frequency range for the beam parameters in Table 2 ($f=\omega/2\pi$). These eigenfrequencies can be obtained from the relations $f_n=\sqrt{B/(\rho S)}k_n^2/2\pi$; $k_n=n\pi/L\ \forall n=1\cdots\infty$ (see, e.g., Refs. [16,17]). The condition $\det(\hat{\mathbf{T}}^G)\neq 0$ will be assumed from now on, i.e., the subsequent results will be valid for $f\neq f_n$.

Proving (19a) requires some lengthy but straightforward algebra. Only the main steps and an intermediate result will be given here for the $(\hat{\mathbf{T}}^G)^{-1}|_{14}=0$ case, since $(\hat{\mathbf{T}}^G)^{-1}|_{41}=0$ has to be dealt

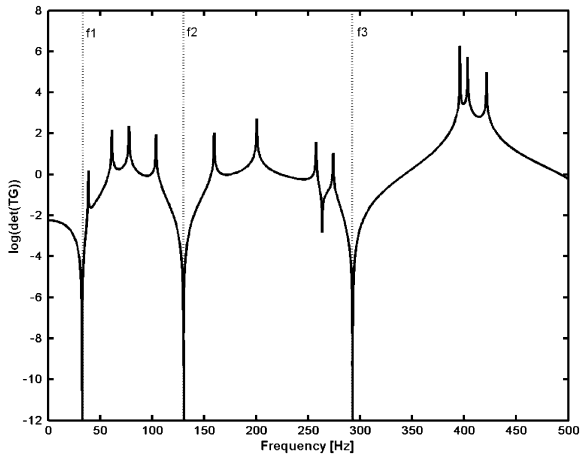

Fig. 3. Logarithm of $\det(\hat{T}^G)$ vs. frequency. The determinant vanishes at the simply supported beam eigenfrequencies f_1, f_2 and f_3.

Table 2
Beam parameters

Description	Variable	Value
Beam length	L	10 m
Beam radius	R	0.05 m
Beam density	ρ	$7800\,\mathrm{kg\,m^{-3}}$
Young's modulus	E	$21\times10^{10}\,\mathrm{kg\,m^{-1}\,s^{-2}}$

in the same way. It has to be proven that

$$(\hat{\mathbf{T}}^G)^{-1}|_{14} = \det(\hat{\mathbf{T}}^G)\left[\hat{T}^G_{12}\underbrace{(\hat{T}^G_{24}-\hat{T}^G_{23}\hat{T}^G_{34})}_{A}+\hat{T}^G_{13}\underbrace{(\hat{T}^G_{34}-\hat{T}^G_{32}\hat{T}^G_{24})}_{B}+\hat{T}^G_{14}\underbrace{(\hat{T}^G_{23}\hat{T}^G_{32}-1)}_{C}\right]=0. \quad (20)$$

As it has been assumed that $\det(\hat{\mathbf{T}}^G)\neq 0$, it will suffice to prove that the bracketed term is equal to zero. Substituting (13), (14), (16) and (17) into (18) and then into (20), this yields after some calculations to

$$\begin{aligned} A = {} & \sinh(kL)\sin(kL) \\ & \times \frac{[\cos(kx_2)\sinh(kx_2)-\sin(kx_2)\cosh(kx_2)]}{[\sinh(kL)\sin(kx_2)\sinh(k(x_2-L))-\sin(kL)\sinh(kx_2)\sinh(k(x_2-L))]} \\ & \times \frac{[\sinh(k(x_3-L))\cos(k(x_2-L))-\sin(k(x_3-L))\cosh(k(x_2-L))]}{[\sin(kL)\cosh(kx_2)\cosh(k(x_2-L))-\sinh(kL)\cos(kx_2)\cos(k(x_2-L))]}, \end{aligned} \quad (21)$$

$$B = \frac{1}{k}\sinh(kL)\sin(kL) \times \frac{[\cos(kx_2)\sinh(kx_2) - \sin(kx_2)\cosh(kx_2)]}{[\sin(kL)\cosh(kx_2)\cos(k(x_2-L)) - \sinh(kL)\cos(kx_2)\cos(k(x_2-L))]} \times \frac{[\sin(k(x_3-L))\sinh(k(x_2-L)) - \sinh(k(x_3-L))\sin(k(x_2-L))]}{[\sinh(kL)\sin(kx_2)\sin(k(x_2-L)) - \sin(kL)\sinh(kx_2)\sinh(k(x_2-L))]}, \quad (22)$$

$$C = \sinh(kL)\sin(kL) \times \frac{[\sin(kx_2)\cosh(kx_2) - \cos(kx_2)\sinh(kx_2)]}{[\sin(kL)\cosh(kx_2)\cos(k(x_2-L)) - \sinh(kL)\cos(kx_2)\cos(k(x_2-L))]} \times \frac{[\sin(k(x_2-L))\cosh(k(x_2-L)) - \sinh(k(x_2-L))\cos(k(x_2-L))]}{[\sin(kL)\sinh(kx_2)\sinh(k(x_2-L)) - \sinh(kL)\sin(kx_2)\sin(k(x_2-L))]}. \quad (23)$$

In addition it follows from (18) that

$$\hat{T}_{12}^{G} = \frac{\sin(kL)\sinh(k(x_2-L))\sinh(kx_1) - \sinh(kL)\sin(k(x_2-L))\sin(kx_1)}{\sin(kL)\sinh(kx_1)\sinh(k(x_1-L)) - \sinh(kL)\sin(kx_1)\sin(k(x_1-L))}, \quad (24)$$

$$\hat{T}_{13}^{G} = k\frac{\sin(kL)\cosh(k(x_2-L))\sinh(kx_1) - \sinh(kL)\cos(k(x_2-L))\sin(kx_1)}{\sin(kL)\sinh(kx_1)\sinh(k(x_1-L)) - \sinh(kL)\sin(kx_1)\sin(k(x_1-L))}, \quad (25)$$

$$\hat{T}_{14}^{G} = \frac{\sin(kL)\sinh(k(x_3-L))\sinh(kx_1) - \sinh(kL)\sin(k(x_3-L))\sin(kx_1)}{\sin(kL)\sinh(kx_1)\sinh(k(x_1-L)) - \sinh(kL)\sin(kx_1)\sin(k(x_1-L))}. \quad (26)$$

Substituting (21)–(26) into (20) and carrying out some more calculations gives

$$\hat{T}_{12}^{G}A + \hat{T}_{13}^{G}B + \hat{T}_{14}^{G}C = 0 \quad (27)$$

and hence the expected result $\hat{T}_{14}^{D} = 0$ is obtained.

Condition (19b) can be shown to be fulfilled arguing by contradiction, i.e., by assuming that these transfer functions have a zero value and then finding an example that denies this assumption. The following case will prove useful for this purpose. The values $\{x_1 = L/4, x_2 = 3L/8, x_3 = 7L/8\}$ are selected for the three beam points and use is made again of the beam parameters listed in Table 2.

The GTFs calculated from (18) for the above example and their corresponding DTFs, obtained from Eq. (7) together with relationships (8a) and (b), are shown in Fig. 4. The values of $20\log_{10}(|\hat{T}_{ij}^{G,D}|) \quad i,j = 1,\ldots,4$ are plotted for a frequency range of [0,500] Hz. It can be checked that condition (19b) fulfils. That is, from Figs. 4a, d, m and p it can first be observed that while $20\log_{10}(|\hat{T}_{ii}^{G}|) = 0$ as $\hat{T}_{ii}^{G} = 1, \quad \forall i = 1,\cdots,4$, the logarithm of $\hat{T}_{ii}^{D}, \quad \forall i = 1,\cdots,4$, are non-zero and well-defined functions. Moreover, it is clearly seen from Figs. 4b, c, e, f, h, i, k, l, n and o that $\hat{T}_{ij}^{D} \neq 0 \quad i,j = 1,\cdots,3, \quad i,j = 2,\cdots,4$ with $i \neq j$. On the other hand, and as expected, $\hat{T}_{41}^{D}$ and $\hat{T}_{14}^{D}$ do not appear in Figs. 4g and j as they are zero and consequently their logarithm is at $-\infty$. On the contrary $\hat{T}_{41}^{G}$ and $\hat{T}_{14}^{G}$ are well-defined functions with $\hat{T}_{41}^{G}, \hat{T}_{14}^{G} \neq 0$. It also has to be pointed out that the peak and dip values in all graphs in Fig. 4 should go to infinity although this is not seen due to resolution effects. The peaks of the GTFs in Fig. 4 occur at the antiresonances of the receptances belonging to the denominators of the GTFs expression (18). Conversely, the dips take place at the antiresonances of the cross-receptances in the numerator of the GTFs. This can be clearly seen in Fig. 5, where the signal–signal GTF between x_1 and x_2, $\hat{T}_{12}^{G}$, the receptance at x_1, $\hat{U}_F(x_1,x_1)$ and

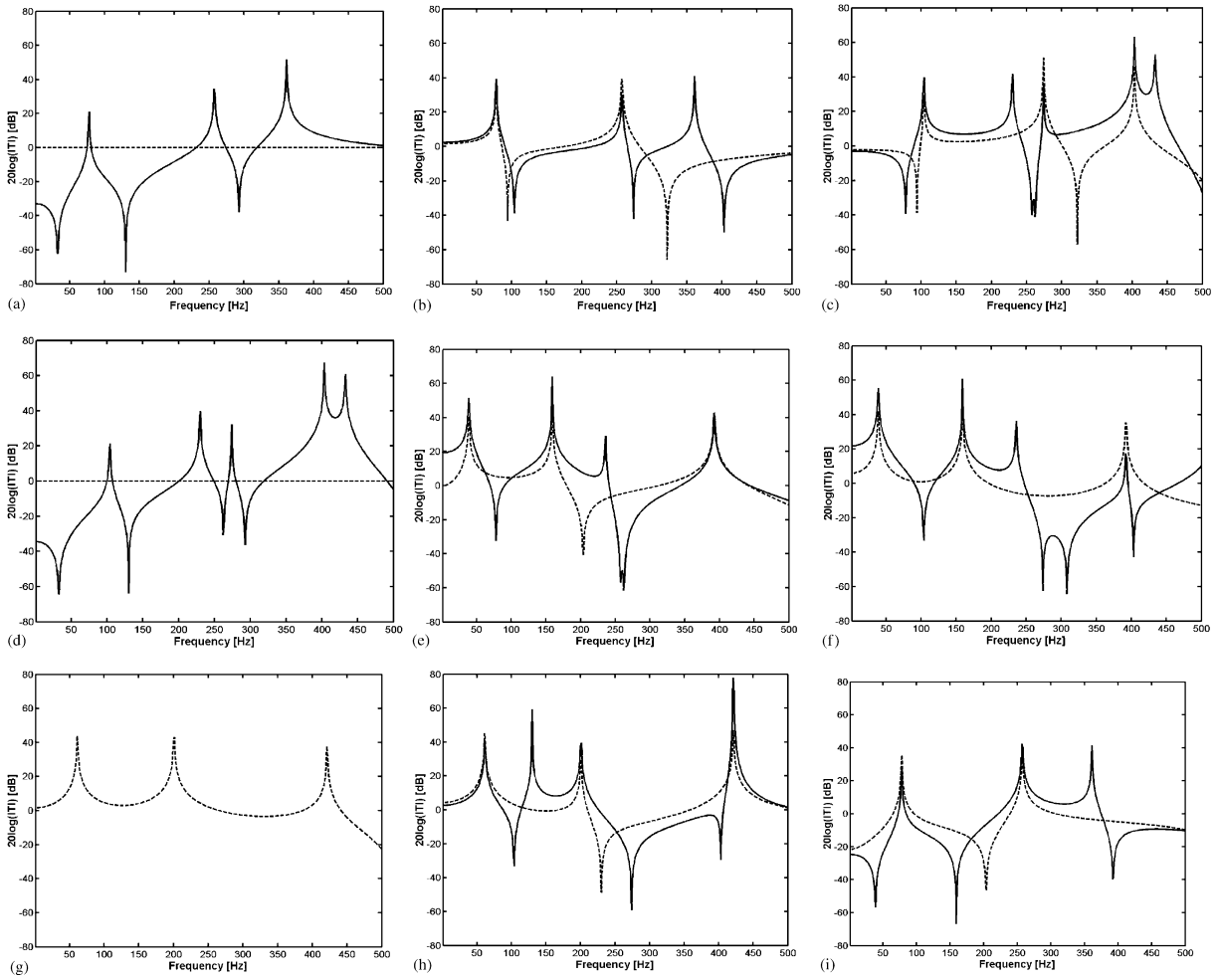

Fig. 4. GTFs and DTFs for the beam example. (a) $\hat{T}_{11}^{D}$ continuous (—), $\hat{T}_{11}^{G}$ dashed (––); (b) $\hat{T}_{12}^{D}$ continuous (—), $\hat{T}_{12}^{G}$ dashed (––); (c) $\hat{T}_{21}^{D}$ continuous (—), $\hat{T}_{21}^{G}$ dashed (––); (d) $\hat{T}_{22}^{D}$ continuous (—), $\hat{T}_{22}^{G}$ dashed (––); (e) $\hat{T}_{31}^{D}$ continuous (—), $\hat{T}_{31}^{G}$ dashed (––); (f) $\hat{T}_{32}^{D}$ continuous (—), $\hat{T}_{32}^{G}$ dashed (––); (g) $\hat{T}_{41}^{D}$ continuous (—), $\hat{T}_{41}^{G}$ dashed (––); (h) $\hat{T}_{42}^{D}$ continuous (—), $\hat{T}_{42}^{G}$ dashed (––); (i) $\hat{T}_{13}^{D}$ continuous (—), $\hat{T}_{13}^{G}$ dashed (––); (j) $\hat{T}_{14}^{D}$ continuous (—), $\hat{T}_{14}^{G}$ dashed (––); (k) $\hat{T}_{23}^{D}$ continuous (—), $\hat{T}_{23}^{G}$ dashed (––); (l) $\hat{T}_{24}^{D}$ continuous (—), $\hat{T}_{24}^{G}$ dashed (––); (m) $\hat{T}_{33}^{D}$ continuous (—), $\hat{T}_{33}^{G}$ dashed (––); (n) $\hat{T}_{43}^{D}$ continuous (—), $\hat{T}_{43}^{G}$ dashed (––); (o) $\hat{T}_{34}^{D}$ continuous (—), $\hat{T}_{34}^{G}$ dashed (––); (p) $\hat{T}_{44}^{D}$ continuous (—), $\hat{T}_{44}^{G}$ dashed (––).

the cross-receptance between x_1 and x_2, $\hat{U}_F^{>}(x_2, x_1)$ are plotted. While $\hat{U}_F(x_1, x_1)$ and $\hat{U}_F^{>}(x_2, x_1)$ have their peaks at the simply supported beam eigenfrequencies, the peaks of $\hat{T}_{12}^{G}$ correspond to the antiresonances of $\hat{U}_F(x_1, x_1)$. It can also be seen that the dips of $\hat{T}_{12}^{G}$ correspond to the antiresonances of $\hat{U}_F^{>}(x_2, x_1)$. This is an expected result as $\hat{T}_{12}^{G} = \hat{U}_F^{>}(x_2, x_1)/\hat{U}_F(x_1, x_1)$. On the other hand, it can be observed that the peaks and dips of the DTFs in Fig. 4 do not necessarily coincide with those of the GTFs. This is also an expected result: as the DTF between x_i and x_j represent the transfer function when the remaining $x_k \ \forall k \neq i, j$ are blocked, the eigenfunctions, eigenfrequencies and antiresonances of the beam with these additional restrictions will differ from the original ones. Consequently, the DTF peak and dip values will not generally coincide with those from the corresponding GTFs.

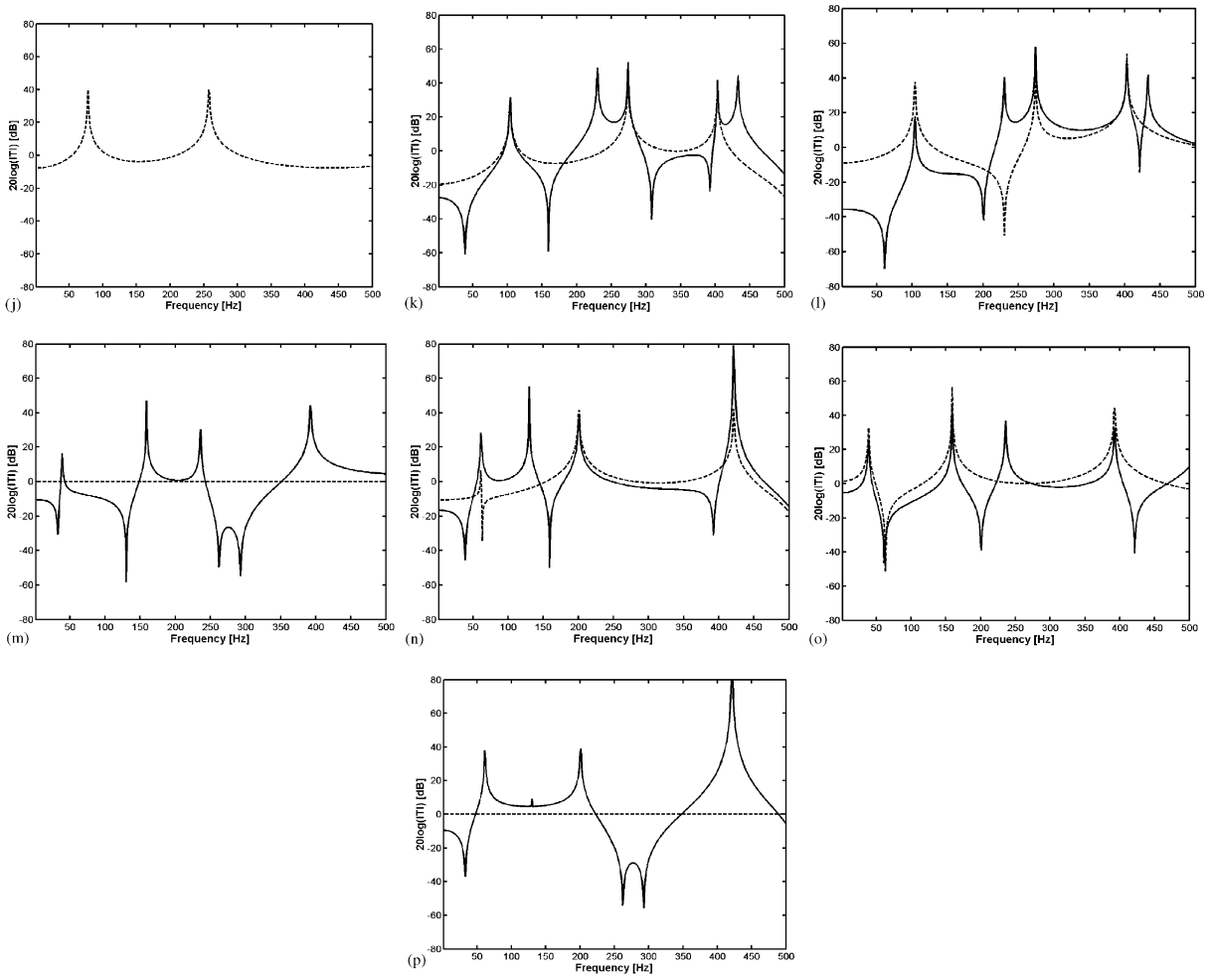

Fig. 4 (*continued*).

6. Signal reconstruction

6.1. The FTF method reconstruction

From (13), (14), (16) and (17) the receptance matrix can be built. This matrix is given by

$$\begin{array}{llll} \hat{T}_{11}^{GF} = \hat{U}_F(x_1,x_1), & \hat{T}_{12}^{GF} = \hat{U}_F^{>}(x_2,x_1), & \hat{T}_{13}^{GF} = \hat{W}_F^{>}(x_2,x_1), & \hat{T}_{14}^{G} = \hat{U}_F^{>}(x_3,x_1), \\ \hat{T}_{21}^{GF} = \hat{U}_F^{<}(x_1,x_2), & \hat{T}_{22}^{GF} = \hat{U}_F(x_2,x_2), & \hat{T}_{23}^{GF} = \hat{W}_F(x_2,x_2), & \hat{T}_{24}^{GF} = \hat{U}_F^{>}(x_3,x_2), \\ \hat{T}_{31}^{GF} = \hat{U}_M^{<}(x_1,x_2), & \hat{T}_{32}^{GF} = \hat{U}_M(x_2,x_2), & \hat{T}_{33}^{GF} = \hat{W}_M(x_2,x_2), & \hat{T}_{34}^{GF} = \hat{U}_M^{>}(x_3,x_2), \\ \hat{T}_{41}^{GF} = \hat{U}_F^{<}(x_1,x_3), & \hat{T}_{42}^{GF} = \hat{U}_F^{<}(x_2,x_3), & \hat{T}_{43}^{GF} = \hat{W}_F^{<}(x_2,x_3), & \hat{T}_{44}^{GF} = \hat{U}_F(x_3,x_3). \end{array} \tag{28}$$

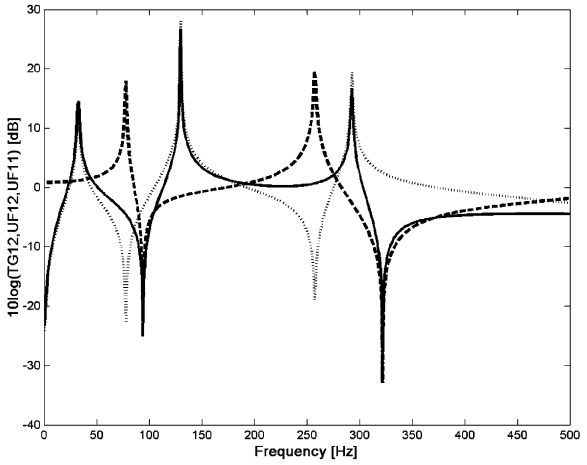

Fig. 5. Global Transfer Function $\hat{T}_{12}^{G}$ dashed (– –), cross-receptance $U_F(x_2, x_1)$ continuous (—), receptance $U_F(x_1, x_1)$ dotted (···).

In the case of a known operational external vector acting on the beam, $\hat{\mathbf{f}}^{ext}(\omega)$, the operational signal at any subsystem can be obtained from the following product:

$$\hat{\mathbf{s}} = \mathbf{T}^{GF\mathrm{T}}\hat{\mathbf{f}}^{ext}. \tag{29}$$

Eq. (29) contains the key information of the FTF method as it allows one to obtain the operational signal at any subsystem in terms of the contributions of the various forces acting on the beam. That is, the signal at i, $\hat{s}_i(\omega)$, can be expressed as the summation of the various force contributions $T_{ji}^{GF}f_j^{ext}\ \ \forall j = 1, \ldots, 4$. In practical applications of the FTF method, measuring the matrix receptance generally poses no difficulties. However, several problems are commonly found when trying to obtain the forces acting on the system under the desired operational conditions. Hence, much development of the FTF method has been precisely focused in finding ways of obtaining these operational forces. However, no further information will given here concerning these and other aspects of the FTF method as it is a widely implemented and well-known method. Only an example of application to the beam case is given here for comparison with the GTDT approach to the problem.

It is assumed for simplicity that the following frequency-independent and arbitrary chosen operational external force vector is acting on the beam:

$$\hat{\mathbf{f}}^{ext} = (3 \times 10^{-2}\mathrm{e}^{\mathrm{i}\theta_1}, 1 \times 10^{-5}\mathrm{e}^{\mathrm{i}\theta_2}, 1 \times 10^{-1}\mathrm{e}^{\mathrm{i}\theta_3}, 7 \times 10^{-3}\mathrm{e}^{\mathrm{i}\theta_4})^{\mathrm{T}} \tag{30}$$

with $\theta_1 = 0^\circ, \theta_2 = 45^\circ,\ \theta_3 = 115^\circ$ and $\theta_4 = 75^\circ$. The force contributions to the signal at any subsystem can then be found from (29). The results are respectively given in Figs. 6a–d for subsystems 1,2,3 and 4. The left-side figures represent $20\log_{10}|T_{ji}^{GF}\hat{f}_j^{ext}|$, i.e., the squared moduli in a logarithmic scale ((dB) ref 1 m), while the right-side figures represent the respective phases in degrees. It can be observed, as usual, that the peaks of the signal at any subsystem are located at the beam eigenfrequencies. This is also true for the peaks of the various force contributions. On the other hand, the main contributors to the overall signal at any subsystem are the force $\hat{f}_1^{ext}$ and the torque $\hat{f}_3^{ext}$. It can also be seen from the modulus plots in Fig. 6 that the force contributions do

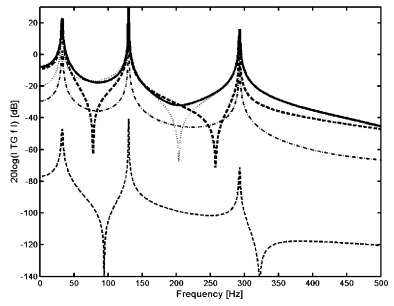

(a) Subsystem 1: overall signal and force contribution moduli

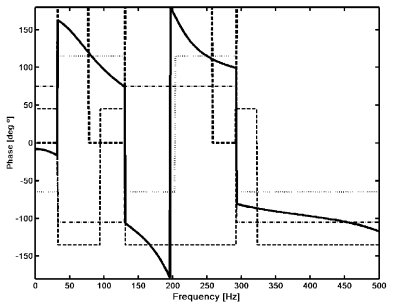

(a) Subsystem 1: overall signal and force contribution phases

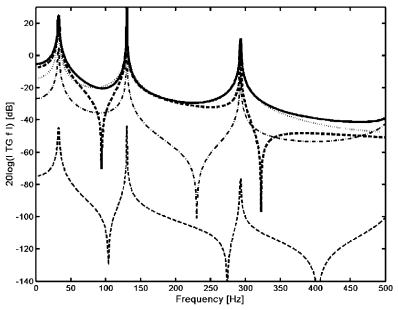

(b) Subsystem 2: overall signal and force contribution moduli

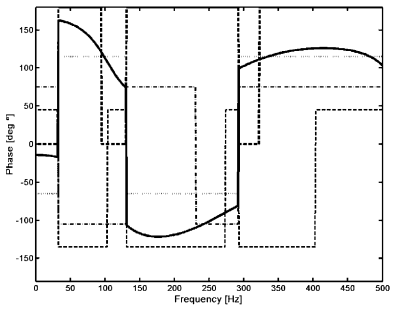

(b) Subsystem 2: overall signal and force contribution phases

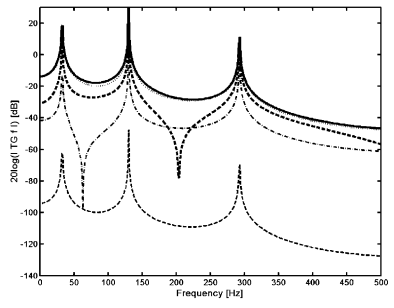

(c) Subsystem 3: overall signal and force contribution moduli

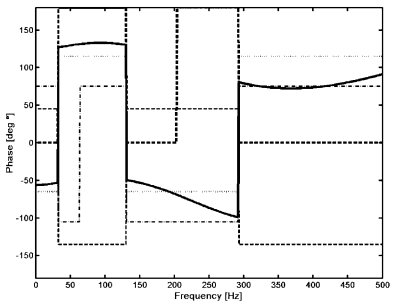

(c) Subsystem 3: overall signal and force contribution phases

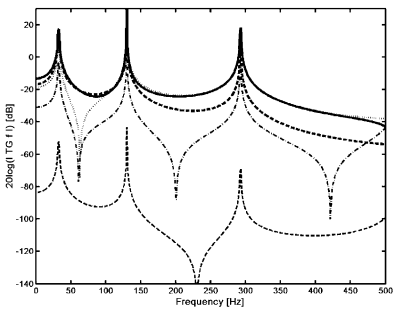

(d) Subsystem 4: overall signal and force contribution moduli

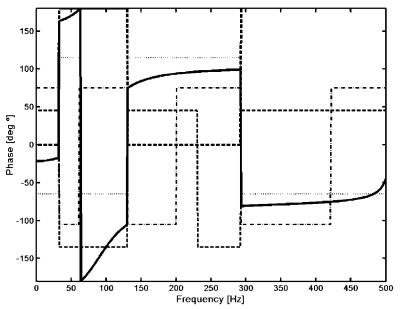

(d) Subsystem 4: overall signal and force contribution phases

Fig. 6. Force contributions (modulus (dB) and phase (deg)): Overall signal at the ith subsystem, $\hat{s}_i$, continuous (—); subsystem 1 force contribution to i, $\hat{T}_{1i}^{G}\hat{f}_1^{ext}$, dashed bold (– –); subsystem 2 force contribution to i, $\hat{T}_{2i}^{G}\hat{f}_2^{ext}$, dashed (– –); subsystem 3 force contribution to i, $\hat{T}_{3i}^{G}\hat{f}_3^{ext}$, dotted (⋯); subsystem 4 force contribution to i, $\hat{T}_{4i}^{G}\hat{f}_4^{ext}$, dotted–dashed(· –).

not generally surpass the overall signal value. This is true except for some frequency ranges that change from figure to figure. For instance, in Fig. 6a the force contribution from subsystem 3 slightly exceeds the overall signal at subsystem 1 in the approximate range of [70 130] Hz. The force contribution from subsystem 1 does so in the approximate range of [130 210] Hz. This can be understood from Fig. 6b where it can be observed that these frequency ranges correspond to changes in the relative phase between subsystem 1 and 3 force contributions yielding the appropriate signal cancellations. Similar results can be found for the remaining Figs. 6b–d although the phase effects remain of little influence for this particular example.

6.2. The GTDT method reconstruction

In the second step of the GTDT method, the signal at any subsystem is obtained by means of Eq. (10). This equation gives the following result for subsystem 2:

$$\hat{s}_2 = \hat{T}^D_{12}\hat{s}_1 + \hat{T}^D_{32}\hat{s}_3 + \hat{T}^D_{42}\hat{s}_4 + \hat{T}^D_{22}\hat{s}^{ext}_2 \tag{31}$$

or the following one for subsystem 4:

$$\hat{s}_4 = \hat{T}^D_{14}\hat{s}_1 + \hat{T}^D_{24}\hat{s}_2 + \hat{T}^D_{34}\hat{s}_3 + \hat{T}^D_{44}\hat{s}^{ext}_4 = \hat{T}^D_{24}\hat{s}_2 + \hat{T}^D_{34}\hat{s}_3 + \hat{T}^D_{44}\hat{s}^{ext}_4, \tag{32}$$

where in the last equality the before proven result $\hat{T}^D_{14} = 0$ has been used. Analogous results are obtained for the remaining subsystems 1 and 3. Thus, it can be seen that the overall operational signal at any subsystem is given in terms of the contributions $\hat{T}^D_{ji}s_j$ of all the remaining subsystems j, with $j \neq i$, and the contribution due to the external signal at i, $\hat{T}^D_{ii}s^{ext}_i$.

By means of Eq. (29), the operational signal vector when the force vector (30) is acting on the beam can be calculated. This vector will be frequency dependent and, although for the beam example is obtained through (29) and (30), it will be a measured quantity in practical applications of the method. Measuring the operational signal vector is usually much easier than measuring the operational force vector.

Results for the beam example are, respectively, shown in Figs. 7a–d for subsystems 1,2,3 and 4. Similar to Fig. 6, the left-side figures represent $20\log_{10}|T^D_{ji}\hat{s}_j|$ and $20\log_{10}|T^D_{ii}\hat{s}^{ext}_i|$, i.e., the squared moduli in a logarithmic scale ((dB) ref 1 m), while the right-side figures represent the respective phases in degrees. Obviously, it can be first observed that the overall operational signal (modulus and phase) for all subsystems in Figs. 7a–d are equal to those in Fig. 6a–d. However, the factorization in terms of subsystem signal contributions is absolutely different from the factorization based on subsystem force contributions. For example, while every plot in Fig. 6 has contributions from the four network subsystems, in Fig. 7a there is no contribution from subsystem 4 because $\hat{T}^D_{41} = 0$. Likewise there is no contribution from subsystem 1 in Fig. 7d because $\hat{T}^D_{14} = 0$. On the other hand, note that unlike the subsystem force contributions in Fig. 6, the subsystem signal contributions do not have peaks at the beam eigenfrequencies only. This is a straightforward consequence of the GTFs and DTFs shapes discussed in Section 5. Moreover, the moduli of the various signal contributions at one subsystem often surpasses its overall signal level. Only appropriate relations of the signal contribution relative phases allow the necessary cancellations to obtain the observed overall signal. Yet this last result is not to be seen as a general difference between the FTF method and the GTDT one, but as an outcome for this particular problem at hand. It can also be seen in Figs. 7a–d that the relative influence of the signal

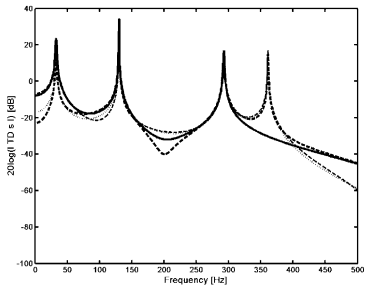

(a) Subsystem 1: overall signal and signal contribution moduli

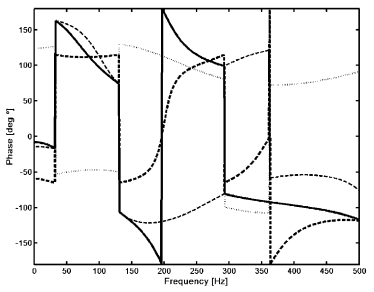

(a) Subsystem 1: overall signal and signal contribution phases

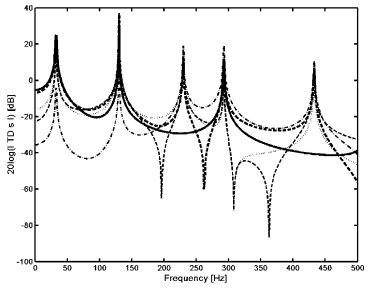

(b) Subsystem 2: overall signal and signal contribution moduli

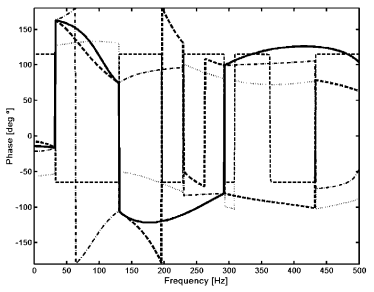

(b) Subsystem 2: overall signal and signal contribution phases

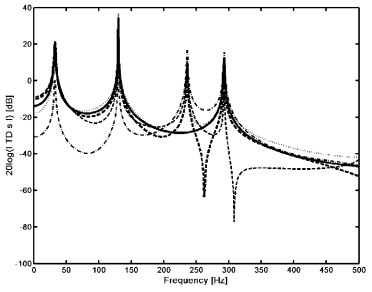

(c) Subsystem 3: overall signal and signal contribution moduli

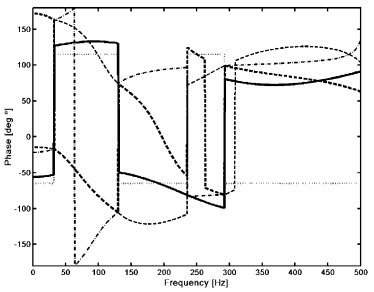

(c) Subsystem 3: overall signal and signal contribution phases

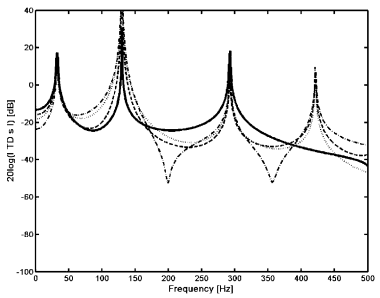

(d) Subsystem 4: overall signal and signal contribution moduli

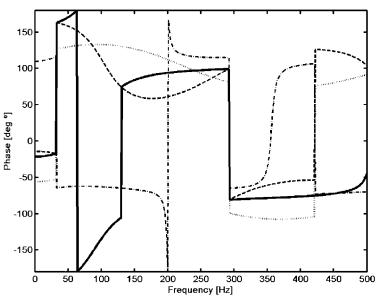

(d) Subsystem 4: overall signal and signal contribution phases

Fig. 7. Signal contributions (modulus (dB) and phase (deg)): Overall signal at the ith subsystem, $\hat{s}_i$, continuous (—); subsystem 1 signal contribution to i, $\hat{T}^D_{1i}\hat{s}_1$, dashed bold (– –); subsystem 2 signal contribution to i, $\hat{T}^D_{2i}\hat{s}_2$, dashed (– –); subsystem 3 signal contribution to i, $\hat{T}^D_{3i}\hat{s}_3$, dotted (···); subsystem 4 signal contribution to i, $\hat{T}^D_{4i}\hat{s}_4$, dotted-dashed($\cdot$ –). (it is assumed in the notation that $\hat{T}^D_{ji}\hat{s}_j$ is to be identified with $\hat{T}^D_{ii}\hat{s}^{ext}_i$ if $i = j$).

contributions for a given subsystem can change considerably with the frequency range. Nevertheless, a detailed discussion on this point for every subsystem and frequency range will not be carried out because the procedure is standard and will not shed extra light on the way the GTDT method works.

6.2.1. Discussion

When the GTDT method is applied in practical situations, each subsystem, or small group of subsystems is intended to represent the behaviour of a physical entity (see example in Section 2 and Fig. 1). This can be done in the low frequency range as well as in the mid-high frequency range, the variability of these ranges usually depending on the particular problem at hand. Intermediate situations generally require some previous numerical treatment to the application of the second step of the method, such as the singular value decomposition technique. This allows one to discriminate if Eq. (10) is needed for the signal reconstruction or if instead an energetic analogue equation is to be used. Moreover, under the energetic assumption, the GTDT method also brings the possibility to factorize any global path linking two subsystems, in terms of path subgroups built from the union of various direct links among subsystems [10]. The factorization by means of the DTFs and subsystem signal contributions allow prediction of how design modifications on one subsystem may affect any other one. This can be done once the new DTFs from the modified subsystem to the remaining ones are calculated and/or if some prediction on its new signal level can be approximated (remember that only DTFs from directly linked subsystems will have a non-zero value). Although in some cases this may seem quite a difficult task, it has been found in practical implementations that even rough estimations of the modified DTFs and subsystem signals can yield good results and predictions.

Finally, it is worthwhile to mention that a central point concerning the practical implementation of the GTDT method (and indeed the FTF method) is the accurate selection of subsystems. For instance, consider again the railway carriage example in Fig. 1. It would be impossible to reconstruct the signal at M if some subsystem (e.g., L1) was omitted. Conversely, if all subsystems were taken into account and the reconstructed signal at M was different from the measured one, this could be indicative of some air leakage problem. The selection of subsystems in the GTDT method also depends on the type of information one desires to obtain. If in the railway carriage example the connection points information was of no interest, it would be possible to work with a reduced five-dimensional network (microphone M, the lateral L1, the lateral L2, the roof R and the floor F) instead of working with the general seven-dimensional one.

7. Conclusions

In this paper, the transmission of bending waves between three points $x_1 < x_2 < x_3$ in a finite simply supported elastic beam has been studied in the framework of the GTDT method of transmission path analysis. The intention was to clarify how the method works, using this example.

The displacements at x_1, x_2 and x_3 have been, respectively, chosen as subsystems 1, 2 and 4 of a four-dimensional discrete network, being the rotation at x_2 the subsystem 3. Concerning the first step of the method, it has been shown that the Direct Transfer Function, $\hat{T}^D_{14}$, is zero for every

frequency while the Global Transfer Function, $\hat{T}_{14}^{G}$, is non-zero. This has shown that the DTF matrix acts as a connectivity matrix because it quantifies the physically intuitive and well-known result that no wave can be transmitted from x_1 to x_3 without inducing either a displacement or a rotation at x_2. The DTF connectivity matrix is not a measurable quantity but the paper has shown how it can be calculated from measurable quantities such as the GTFs.

With regards to the second step of the method, it has been shown how the operational signal at any subsystem can be recovered from the signal of all the other subsystems plus the external excitation acting on it. This procedure allows detection of the subsystems to be modified in order to reduce the signal at a given location and also allows prediction of how design modifications may affect the signal level at any subsystem. Moreover, it avoids the necessity to measure operational forces.

Acknowledgements

The authors gratefully acknowledge R. Codina from UPC (Universitat Politècnica de Catalunya) for valuable comments and discussions.

Appendix A. Force receptance

There are several ways of finding the exact Green function associated to Eq. (12) in text, all of them yielding more or less to the same amount of calculations. The wanted exact Green function will be found here by explicit construction and will have the form

$$\hat{U}_F(x,x_0) \equiv G(x,x_0) = \begin{cases} A^{<}\mathrm{e}^{kx} + B^{<}\mathrm{e}^{-kx} + C^{<}\mathrm{e}^{\mathrm{i}kx} + D^{<}\mathrm{e}^{-\mathrm{i}kx} \equiv G^{<}(x,x_0), & x<x_0, \\ A^{>}\mathrm{e}^{kx} + B^{>}\mathrm{e}^{-kx} + C^{>}\mathrm{e}^{\mathrm{i}kx} + D^{>}\mathrm{e}^{-\mathrm{i}kx} \equiv G^{>}(x,x_0), & x>x_0, \end{cases} \tag{A.1}$$

where $G^{<}(x,x_0)$ and $G^{>}(x,x_0)$ are solutions of the homogeneous equation $\partial_x^4\hat{U}_F - k^4\hat{U}_F = 0$, respectively, at $x<x_0$ and $x>x_0$. $A^{<}, A^{>}, B^{<}, B^{>}, C^{<}, C^{>}, D^{<}, D^{>}$ are constants depending on x_0 that have to be determined from the boundary conditions of the problem and from the continuity requisites that the Green function has to fulfil.

The boundary conditions for the simply supported beam allow no displacement at the end points. Moreover, no moments can be applied at these points. These conditions applied to (A.1) read

$$G(0,x_0) = 0, \text{ No displacement at } x=0, \tag{A.2a}$$

$$G(L,x_0) = 0, \text{ No displacement at } x=L, \tag{A.2b}$$

$$\partial_x^2 G(0,x_0) = 0, \text{ No moment at } x=0, \tag{A.2c}$$

$$\partial_x^2 G(L,x_0) = 0, \text{ No moment at } x=L. \tag{A.2d}$$

Requiring the Green function to satisfy (A.2a)–(A.2d) the following relationships among the unknown constants can be easily found:

$$A^{<} = -B^{<}, \quad C^{<} = -D^{<}, \quad A^{>} = -B^{>}\mathrm{e}^{-2kL}, \quad C^{>} = -D^{>}\mathrm{e}^{-2\mathrm{i}kL}. \tag{A.3}$$

Substituting (A.3) into (A.1), and renaming the constants where appropriate, yields

$$\hat{U}_F(x,x_0) \equiv G(x,x_0) = \begin{cases} A^< \sinh(kx) + C^< \sin(kx) \equiv G^<(x,x_0), & x < x_0, \\ A^> \sinh(k(x-L)) + C^> \sin(k(x-L)) \equiv G^>(x,x_0), & x > x_0, \end{cases} \tag{A.4}$$

The following notation will be adopted:

$$\begin{aligned} G^{\lessgtr}(x_0^{\mp},x_0) &\equiv \lim_{\substack{x\to x_0 \\ x^{\lessgtr}x_0}} G(x,x_0) = G^{\lessgtr}(x_0,x_0), \\ \partial_x^i G^{\lessgtr}(x_0^{\mp},x_0) &\equiv \lim_{\substack{x\to x_0 \\ x^{\lessgtr}x_0}} \partial_x^i G(x,x_0) = \partial_x^i G^{\lessgtr}(x_0,x_0). \end{aligned} \tag{A.5}$$

In order to find the remaining constants $A^<, A^>, C^<$ and $C^>$ function (A.4) is required to comply with the following continuity conditions:

$$G^>(x_0^+,x_0) - G^<(x_0^-,x_0) = 0, \text{ Function's continuity at } x = x_0, \tag{A.6a}$$

$$\partial_x G^>(x_0^+,x_0) - \partial_x G^<(x_0^-,x_0) = 0, \text{ First derivative continuity at } x = x_0, \tag{A.6b}$$

$$\partial_x^2 G^>(x_0^+,x_0) - \partial_x^2 G^<(x_0^-,x_0) = 0, \text{ Second derivative continuity at } x = x_0, \tag{A.6c}$$

$$\partial_x^3 G^>(x_0^+,x_0) - \partial_x^3 G^>(x_0^-,x_0) = -1, \text{ Third derivative discontinuity at } x = x_0. \tag{A.6d}$$

Note that condition (A.6d) is responsible for the appearance of a delta function when the fourth derivative is carried out. Requiring (A.4) to satisfy (A.6a)–(A.6d) and taking into account (A.5) the following system of equations can be derived:

$$\begin{bmatrix} \sinh(kx_0) & \sin(kx_0) & -\sinh(k(x_0-L)) & -\sin(k(x_0-L)) \\ \cosh(kx_0) & \cos(kx_0) & -\cosh(k(x_0-L)) & -\cos(k(x_0-L)) \\ \sinh(kx_0) & -\sin(kx_0) & -\sinh(k(x_0-L)) & \sin(k(x_0-L)) \\ \cosh(kx_0) & -\cos(kx_0) & -\cosh(k(x_0-L)) & \cos(k(x_0-L)) \end{bmatrix} \begin{bmatrix} A^< \\ C^< \\ A^> \\ C^> \end{bmatrix} = \begin{bmatrix} 0 \\ 0 \\ 0 \\ -1/k^3 \end{bmatrix} \tag{A.7}$$

the solution of which is given by

$$\begin{aligned} A^< &= \frac{1}{2k^3}\frac{\sinh(k(x_0-L))}{\sinh(kL)}, & C^< &= -\frac{1}{2k^3}\frac{\sin(k(x_0-L))}{\sin(kL)}, \\ A^> &= \frac{1}{2k^3}\frac{\sinh(kx_0)}{\sinh(kL)}, & C^> &= -\frac{1}{2k^3}\frac{\sin(kx_0)}{\sin(kL)}. \end{aligned} \tag{A.8}$$

Substitution of (A.8) into (A.4) finally yields Eq. (13) in text.

Appendix B. Moment receptance

In order to find the solution to Eq. (15) in text, the following well-known result will be used (see, e.g., Ref. [18]): Given a linear partial-differential operator L_x, the solution $\varphi(x)$ to the inhomogeneous equation

$$L_x\varphi(x) = Q(x), \quad x \in \Omega \tag{B.1}$$

can be found once the solution (the Green function) to (B.1) with a delta-function inhomogeneity is known. The solution is given by

$$\varphi(x) = \int_{\Omega} G(x,y)Q(y)\mathrm{d}y + \varphi_h(x), \tag{B.2}$$

where $G(x,y)$ is the solution of

$$L_x G(x,y) = \delta(x-y) \tag{B.3}$$

and $\varphi_h(x)$ is the solution of the associated homogeneous problem $L_x\varphi(x) = 0$. In the case of $G(x,y)$ being the *exact* Green equation of the problem, $\varphi_h(x)$ vanishes and the solution is only given by the integral term in Eq. (B.2).

Applying this result to Eq. (15) in text gives

$$\begin{aligned}\hat{U}_M &= \int_{\Omega} G(x,y)\partial_y\delta(y-x_0)\,\mathrm{d}y \\ &= -\int_{\Omega} \partial_y G(x,y)\delta(y-x_0)\,\mathrm{d}y + \int_{\partial\Omega} G(x,y)\delta(y-x_0)\,\mathrm{d}y \\ &= -\partial_y G(x,y)|_{\substack{x\\ y=x_0}} + G(x,x_0)|_{\partial\Omega} = -\partial_y G(x,y)|_{\substack{x\\ y=x_0}} \equiv -\partial_{x_0} G(x,x_0),\end{aligned} \tag{B.4}$$

where the boundary term has vanished as the Green function fulfils the boundary conditions (A.2a) and (A.2b). Note that the above operations can be performed because the order of derivability of the Green function at hand is higher than the order of the derivative of the delta-function inhomogeneity appearing in Eq. (15).

Applying reasoning (B.1)–(B.4) into (15) and taking into account that the Green function is given by Eq. (13), finally results in Eq. (16) in text.

References

[1] C.J. Dodds, J.D. Robson, Partial coherence in multivariate random processes, *Journal of Sound and Vibration* 42 (1975) 243–249.
[2] J.S. Bendat, Solutions for the multiple input/output problem, *Journal of Sound and Vibration* 44 (3) (1976) 311–325.
[3] J.S. Bendat, System identification from multiple input/output data, *Journal of Sound and Vibration* 49 (3) (1976) 293–308.
[4] J.S. Bendat, A.G. Piersol, *Engineering Applications of Correlation and Spectral Analysis*, Wiley, New York, 1980.
[5] R. Potter, Matrix formulation of multiple and partial coherence, *Journal of the Acoustical Society of America* 61 (1977) 776–781.
[6] I.G. Desanghere, Identification and allocation of noise vibration energy sources using frequency response and coherence functions, in: *Seminar on Localization and Visualization of Acoustic Noise Sources. Signal Processing Techniques including Acoustic Intensity*, Organized by Afdeling Mechanische Produktie en Konstructie, K.U. Leuven, 31 March 1982.
[7] F.X. Magrans, Method of measuring transmission paths, *Journal of Sound and Vibration* 74 (3) (1981) 321–330.
[8] W. Stahel, R.H. van Ligten, J. Gillard, Measuring method to obtain the transmission paths and simultaneous real force contributions in a mechanical linear system, Technical Report *No* 80.21 Lab, Acústico Italiana Keller, 1980.
[9] H.R. Tschudi, The force transmission path method: an interesting alternative concerning demounting tests, Unikeller Conference 91, 1991.

[10] F.X. Magrans, Direct transference applied to the study of room acoustics, *Journal of Sound and Vibration* 96 (1) (1984) 13–21.
[11] E. Kruzins, F. Fricke, The prediction of sound fields in non-diffuse spaces by random walk approach, *Journal of Sound and Vibration* 81 (1982) 549–564.
[12] F.X. Magrans, Definition and calculation of transmission paths within a SEA framework, *Journal of Sound and Vibration* 165 (2) (1993) 277–283.
[13] R.J.M. Craik, *Sound Transmission Through Buildings Using Statistical Energy Analysis*, Gower, London, 1996.
[14] M. Kamiński, M. Ding, W.A. Truccolo, S.L. Bressler, Evaluating causal relationships in neural systems: Granger causality, directed transfer function and statistical assessment of significance, *Biological Cybernetics* 85 (2) (2001) 145–157.
[15] M. Eichler, Granger-causality graphs for multivariate time series, University of Heidelberg, 2002, Preprint.
[16] P.M. Morse, K.U. Ingard, *Theoretical Acoustics*, McGraw-Hill, New York, 1968.
[17] M.C. Junger, D. Feit, *Sound, Structures and their Interaction*, The MIT Press, Cambridge, 1972.
[18] D.G. Crighton, A.P. Dowling, J.E. Ffowcs Williams, M. Heckl, F.G. Leppington, *Modern Methods in Analytical Acoustics*, Springer, Berlin, 1992.